# Tactile rendering of textures by an Electro-Active Polymer device: mimicking Friction-Induced Vibrations

**Livia Felicetti[1-2)*], Eric Chatelet[2)], Antoine Latour[3)], Pierre-Henri Cornuault[4)], Francesco Massi[1)]**

[1)] Dept. of Mechanical and Aerospace Engineering, Sapienza University of Rome, Italy

[2)] Univ Lyon, INSA-Lyon, CNRS UMR5259, LaMCoS, F-69621, France

[3)] Université Grenoble Alpes, CEA LITEN, Avenue des Martyrs 17, 38000 Grenoble, France

[4)] Univ. Bourgogne Franche-Comté, Femto-ST Institute CNRS/UFC/ENSMM/UTBM, Department of Applied Mechanics, 24 rue de l'Epitaphe, Besançon, France

*Corresponding author: felicetti.1607776@studenti.uniroma1.it

ABSTRACT

Starting from the previous analyses of Friction-Induced Vibrations (FIV) and their role in the perception of textures, a tactile rendering device, named PIEZOTACT, has been developed by a thin, lightweight and flexible Electro-Active Polymer (EAP) actuator. The presented signal processing strategy, exploiting the experimentally characterized Transfer Function of the electro-mechanical device, allowed to mimic and accurately reproduce the FIV stimuli obtained from the touch of real textures. An experimental analysis demonstrated that the developed signal processing methodology enables to appropriately reproduce, by the PIEZOTACT device, the tactile stimuli (FIV) measured when touching the real surfaces. A preliminary discrimination campaign, performed on a single subject, validated the device, being the subject able to discriminate the simulated textures with a low number of mistakes, which were consistent with the ones occurred when discriminating the corresponding real surfaces. Moreover, the spectra of the induced vibrations (tactile stimuli) allowed as well to explain the difficulties to discriminate certain textures.

Keywords: tactile mechanical signals, friction-induced vibrations, vibrotactile rendering, tactile perception

## 1. Introduction

Human beings perceive, apprehend and interact with the external world by means of different sensory channels that operate synergistically: the five senses. The recording and rendering of the perceptual stimuli are at the basis of all the communication and human-machine interaction devices.

We currently master the signals that are at the basis of hearing and vision, that can be reproduced by acoustic speakers and visual displays. Acoustic and graphic interfaces are part of our everyday life from decades. On the contrary, the rendering of tactile stimuli is still an open challenge. In this context, the so-called “surface haptics” (i.e. haptics for interactive surfaces [1]) represents a great enhancement of the current human-machine interface technologies and a new channel to interact with virtual environments [1,2]. In our daily life we deal with devices like mobile phones, tablets and videogame controllers, that are already able to deliver some haptic feedbacks, such as vibrations, pulses, bumping and buzzing effects. Recent researches in the field of surface haptics aim to the possibility to render shapes, surface features and textures with computer interfaces, displays, handheld or wearable devices. Tactile rendering will enhance the existing technologies in a countless number of fields, such as online commerce, virtual reality, augmented reality, videogaming, movies, multimedia contents, art, tactile rehabilitation, teleoperation, remote surgery and much else. As well, the social implications of such technologies would be enormous.

Many reviews give an overview of the currently existing studies related to haptic devices and tactile rendering methods [1-4,5]. The most commonly used approaches for rendering shapes and textures include vibrotactile [6-11], electrostatic [12-17] and ultrasonic [18-22] devices. Some studies combine multiple rendering modalities [23,24]. Electrostatic and ultrasonic devices are based on friction modulation [5], while vibrotactile rendering is carried out through mechanical vibrations. In electrostatic devices, modulation of friction is achieved by generating electrostatic attraction forces between the user fingertip and the device surface; ultrasonic devices are based on the air film that is generated between the user fingertip and the vibrating display, when the latter is actuated at ultrasonic frequencies. The vibrotactile approach has long been used for creating tactile buttons or very simple haptic effects, like the ones we are used to in mobile phones and videogame controllers. Recently the possibility of using it to obtain a vibrotactile rendering of textures and fine surface roughness has been explored [6-11]. A data-driven approach is frequently used in vibrotactile rendering as well as in electrostatic and ultrasonic ones [6-10,12-14,18,21,24]. Databases of acceleration, velocity and friction forces measured by scanning real textures are available in literature [25-27]. Another common approach in vibrotactile rendering consists in scanning the surface using a stylus or a rigid tool, equipped with vibration and force transducers, which mediates the contact between finger and texture [6-10,24].

On another hand, in order to be able to render tactile stimuli, the understanding of the mechanisms and the signals that lie at the origin of touch is fundamental. The mechanical stimuli are detected by mechanoreceptors, transduced as electrical signals, carried by nerves, and then decoded by the brain. According to the "duplex theory of tactile perception" [28,29,30], coarse textures can be perceived with the sole static contact between finger and surface, while a sliding motion is required to discriminate finer textures. In fact, when a sliding contact between finger and surface occurs, Friction-Induced Vibrations (FIV) are generated at the contact interface [31,32,33]. A recent line of research is investigating how mechanical stimuli, as the FIV, encode the topographical features of the surfaces, allowing the discriminative perception of textures [33-43]. According to these studies, the acceleration RMS and frequency distribution of the FIV, originated by the fingertip scanning of a texture, show typical features depending on the surface topography, as well as the exploration dynamics, the contact boundary conditions and the fingerprints characteristics. For example, in periodic textures, the fundamental frequency peak of the induced vibrations is given by the ratio between the sliding speed and the smaller wavelength between the one of the fingerprints and the one of the sample roughness. The fingerprints wavelength affects the threshold between coarse and fine textures perception fields [33-38]. A recent work [38] investigated the relation between the topographical characteristics of well-defined sample surfaces and the tribological and dynamical signals obtained by fingertip/surface scanning, correlating them with both the perceptual and the hedonistic feeling of the textures and the related descriptors. According to this study, both the perceptual and the hedonistic sensation of the tested surfaces were mediated by the FIV, which allowed to cluster the textures according to perceptual discrimination categories.

Within this overall framework, the present work reports the development of a technological device and a signal processing strategy for tactile rendering of textured surfaces. Starting from the knowledge acquired on the mechanical stimuli (FIV) and their correlation with tactile perception of textures, an Electro-Active Polymer (EAP) actuator [44,45] has been implemented and driven by an actuation chain. The mechanical stimuli previously measured during the touch of real surfaces have been reproduced thanks to the developed device in order to mimic the touch of the textured surfaces. This kind of printed actuator is characterized by small thickness, small weight and high flexibility, being then suitable to be integrated in tactile displays as well as in wearable devices, such as tactile gloves [44,45,46].

First, the physical device and the data-driven rendering method, which exploits the Transfer Functions of the system to process and reproduce the measured FIV signals, are presented. The developed tactile rendering device has been then used to reproduce the FIV signals measured during the direct sliding contact between the fingertip and a set of real textured samples. A preliminary discrimination campaign on a single subject demonstrated that it was possible to correctly discriminate the textures on the basis of the FIV stimuli, reproduced by the tactile rendering device, with a reduced percentage of errors. Moreover, the analysis of the spectra of the FIV signals has been able to explain the few errors in discrimination of both simulated and real surfaces.

## 2. Materials and Method

### *2.1 Overall approach*

Since the Friction-Induced Vibrations appear to be among the most meaningful signals in order to perceive and discriminate the fine textures [28-43], our goal is to define a methodology to correctly reproduce, by means of an EAP actuator, the FIV previously measured by the sliding interaction between the fingertip and real surfaces.

A preliminary step consisted in establishing a signal processing protocol that allows for reproducing on the fingernail of the subject, when touching the device, the same acceleration signals measured when the finger explores the real surfaces. The determination of the Transfer Function of the electro-mechanical system has been preliminary defined. Then, the signals are processed for driving the EAP and mimicking the FIV stimuli at the origin of the perception. This fundamental step is described in section 3.

After defining and validating the processing for reproducing the FIV signals, a data collection is obtained by measuring the FIV arising when touching a set of different surface samples, chosen between surface textures previously investigated from a perceptual and tribological perspective [38].

The measured mechanical stimuli (FIV) have been then reproduced by the tactile device, developed thanks to the combination of the EAP actuator technology with the developed signal processing strategy. A first attempt to use the developed device for discrimination purpose has been provided by developing a discrimination perceptual campaign on a single subject, testing both the real and the simulated surfaces by the developed tactile device (section 4.2).

While this paper is focused on the development of the tactile device and on the signal processing for mimicking the mechanical stimuli, this preliminary perceptual campaign allowed for validating the approach and for providing feedbacks on the correlation between the spectral features of the FIV and the corresponding capability of discrimination between different textures.

### *2.2. Tactile rendering device: PIEZOTACT*

Our rendering approach consists in measuring the FIV signals generated when sliding the finger on a real surface and reproducing this signal with a vibrotactile actuator. An Electro-Active Polymer (EAP) piezoelectric actuator has been selected to actuate the vibrational signal (Figure 1a). The advantage of exploiting the EAP technology lies in the possibility to integrate the actuator in curved surfaces or in wearable haptic devices due to its flexibility, its lightweight and its small thickness. A certain degree of transparency can be obtained too [44,46], making this kind of actuators also suitable for application in tactile displays and screens. Moreover, the EAP actuator can be realized in many geometries and dimensions. In fact, the actuator is printed with a piezoelectric ink, constituted by the EAP vinylidene fluoride-trifluoroethylene (PVDF-TrFE) copolymers, on a flexible polyethylene naphthalate (PEN) substrate [44,45,46] (Figure 1b). The printed piezo ink film expands when a voltage is applied, resulting in the bending of the actuator, and thus allowing out-of-plane vibrations [44].

The actuator has been held into a plastic ergonomic support produced by additive manufacturing (Figure 1d). The actuator membrane was suspended over a central hole of the support, bounded along its circumference. The shape of the upper part of the support presents a sloped design to allow a comfortable placement of the finger on the actuator. An electronic card (Texas Instruments DRV2667EVM-CT) has been used to drive the EAP actuator. The sound card of a commercial PC (a Lenovo Ideapad 520S-14IKB and a HP Elitebook 830 G5 have been tested, both with good results) has been used as signal generator to send audio signals to the Texas Instruments (TI) card. The assembly constituted by the PC as signal generator, the Texas Instruments card and the EAP actuator, fixed into the support, will be referred in the following as the tactile rendering device, named PIEZOTACT (Fig. 1c).

The actuated vibration can be perceived by placing the fingertip in contact with the actuator surface (Figure 1d). The subject is asked to “touch” the surface with similar force and motion used during active touch of the tested real surfaces (see section 2.4). In fact, in order to provide kinesthetic information to the brain, the subject can mimic the exploration of the real textures by sliding the finger on the actuator membrane. In this case the sliding interaction between the fingertip and the actuator surface needs to be considered. In this preliminary definition of the protocol, the actuator has been covered by a piece of tape, presenting a smooth surface, that has been judged to not influence the perceived vibrations. This assumption has been corroborated by the following tests.

Before exploiting the developed device in order to mimic the FIV stimuli, a signal processing strategy needs to be defined and validated (see section 3) in order to reproduce on the fingernail of the subject the same vibrational signal measured when assessing the real surfaces.

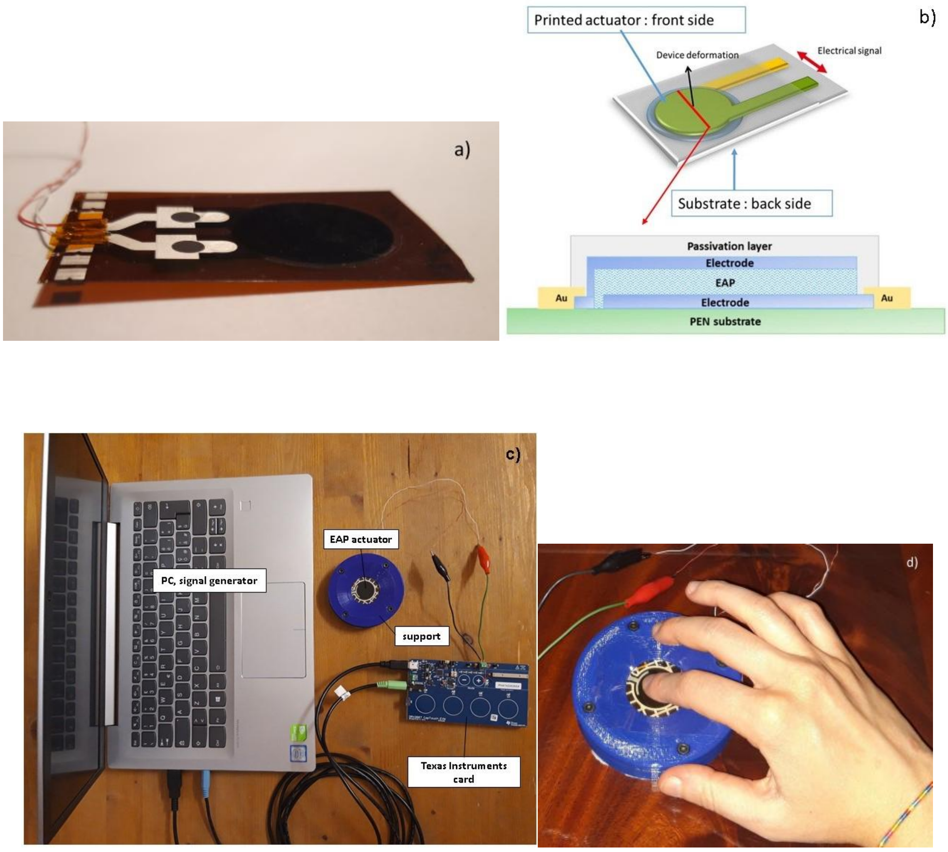


*Figure 1: a) Printed Electro-Active Polymer actuator; b) scheme of the EAP actuator [45]; c) Tactile rendering device PIEZOTACT, constituted by a PC for signal generation, a Texas Instruments card and the EAP actuator, fixed into an ergonomic support. d) The tactile rendering device allows to perceive the vibration by touching the EAP actuator with the finger.*

## 2.3. Surface samples

A set of 12 surface samples with a well-controlled periodic topography [38] have been used as a benchmark. The samples are constituted by rectangular plates made of polyurethane resin (Rencast FC52) with dimensions of 25 x 60 $mm^2$ and a thickness of 3 mm. They were obtained through a multi-step process including photolithography and plasma etching of silicon wafers followed by a moulding/replication process [47]. They show a surface topography characterized by cylindrical “dots” organised in hexagonal pattern (Fig. 2). Their main characteristic dimensions are the height of the dots (H), the diameter of the dots (D) and their spatial period (Sp), i. e. the inter-dots distance. The diameter D ranges between 12 µm and 797 µm, the height H between 14 µm and 38 µm and the spatial period Sp between 13 µm and 607 µm. The surface periodicity is expressed by the equivalent wavelength $\lambda$ = D + Sp ranging between 50 µm and 913 µm. Table 1 reports the topographical data, measured with a 3D variable focus microscope Alicona InfiniteFocus, for the set of samples used in this work. In previous works [38, 47], these samples have been object of a deep investigation, correlating their topographical characterization with the mechanical stimuli (the FIV in particular) and their perceptual and hedonistic feedback (perceptual descriptors).

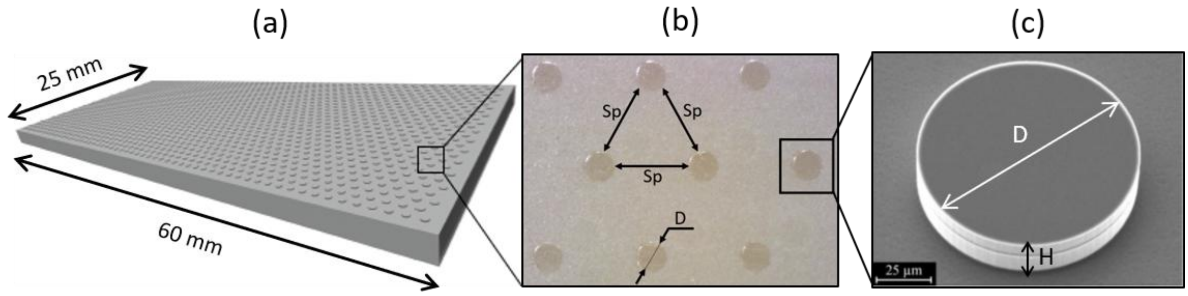


*Figure 2: Surface samples topography and geometric features: (a) scheme of an overall textured sample, (b) optical microscopic observation of a sample surface, (c) scanning electron microscopic observation of a cylindrical dot.*

*Table 1:Ssample topographical dimensions [38]*

| Samples | Height H [µm] | Diameter D [µm] | Spatial period Sp [µm] | Equivalent Wavelength λ [µm] |
|---|---|---|---|---|
| **01** | 27 | 107 | 13 | 120 |
| **02** | 24 | 107 | 53 | 160 |
| **03** | 19 | 22 | 28 | 50 |
| **04** | 38 | 108 | 111 | 218 |
| **05** | 55 | 208 | 109 | 317 |
| **06** | 18 | 71 | 113 | 184 |
| **07** | 14 | 207 | 111 | 318 |
| **08** | 18 | 106 | 607 | 716 |
| **09** | 14 | 207 | 318 | 524 |
| **10** | 27 | 502 | 114 | 616 |
| **11** | 29 | 797 | 116 | 913 |
| **12** | 15 | 12 | 126 | 138 |

## *2.4. Data collection*

In order to record FIV and force data from the finger/surface interaction, the sample surface is mounted on the top of a tri-axial force transducer (Testwell K3D60) and an accelerometer (PCB 352A24, PCB Piezotronics, Inc.) is fixed by wax on the fingernail of the experimenter. The data are acquired by an acquisition system (SIRIUSi - DEWESOFT, based on DualCoreADC® technology with dual 24-bit delta-sigma analog to digital converter (ADC). An anti-aliasing filter on each analog channel achieves a 160 dB dynamic range in time and frequency domains with 200 kHz sampling rate per channel) at a sampling rate of 5kHz.

The acceleration and contact forces are measured, while the experimenter slides the index finger on the sample surface along the proximal direction (Figure 3a). The fingertip/texture interaction is active, that means that the surface is kept motionless and the subject moves him/herself the finger against the sample. Sliding velocity, contact load and finger/surface angle are freely chosen by the subject. However, the experimenter is asked to maintain the normal load in the range between 0.2N and 0.4N, the force range mainly interested in tactile perception. The experimenter strokes the finger across the sample surface several times, lifting the finger between the strokes. While the previous studies were focused on passive touch [33-38] (in order to control the contact parameters for the signal analysis), in this work active touch has been preferred, being the objective the reproduction of perception by a tactile device.

The MATLAB software is used to analyse the data and to perform on the postprocessing of the measured FIV signals (example in Fig. 3b), in order to identify the main spectral features and the most representative FIV features associated to each surface [38]. Finally, the measured signals will be processed (section 3) for driving the EAP device and mimicking the FIV stimuli on the finger of the subject (section 4).

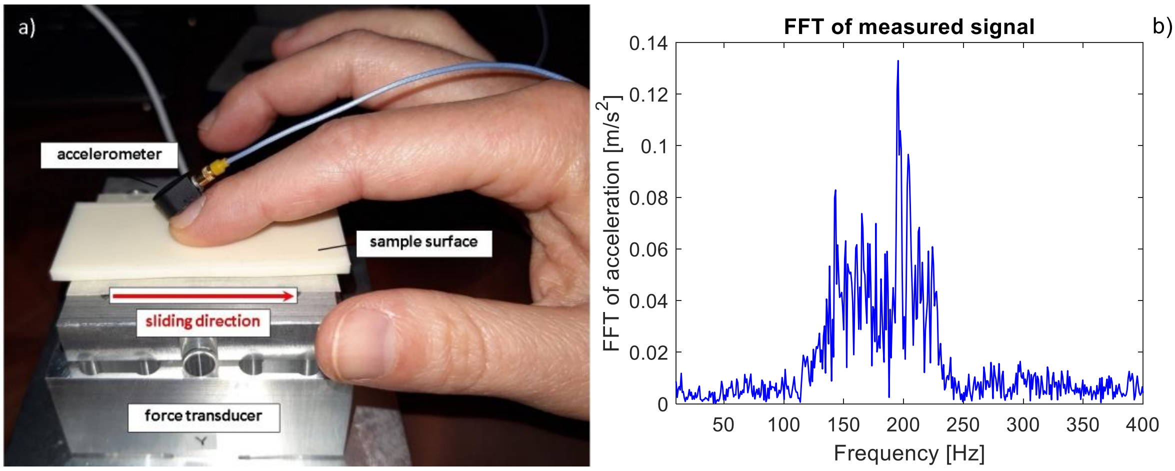


*Figure 3: a) Acceleration and contact forces measurement experimental setup. The sample surface is mounted on the top of the force transducer. The FIV are measured by the accelerometer on the fingernail during the sliding of the finger on the sample surface. b) example of frequency spectrum of the FIV signal measured on the surface sample S02.*

## 3. Signal processing for tactile rendering

### *3.1. Tactile rendering approach*

In order to reproduce with the PIEZOTACT device the vibrational signals measured on the fingernail of the subject, when exploring the real surfaces, the Transfer Function of the tactile rendering device must be considered, accounting for the overall transmission chain: electronics of the audio and TI cards, EAP device and finger structural dynamic response. In fact, if the measured FIV signal is directly sent as input to the tactile rendering device, it is modified by the electro-dynamical system Transfer Function. Here a strategy to correctly reproduce the FIV signal with a tactile rendering device is presented, whatever its Transfer Function is. Once the Transfer Function is experimentally characterized, it will be used to pre-process the FIV signal, measured when touching the real surface, in order to define the input signal that will allow the desired output to be achieved when touching the EAP actuator, i. e. the same signal measured on the fingernail of the subject during the exploration of the real surfaces.

### *3.2. Transfer Function determination*

The PIEZOTACT tactile rendering device allows to actuate a vibration signal that can be perceived by placing the finger on the surface of the actuator. In order to obtain a reproduction of the tactile FIV stimuli on the fingertip, to stimulate the mechanoreceptors by means of the EAP actuator vibration, the acceleration signal measured by the accelerometer fixed on the fingernail is used as a reference. Consequently, the dynamic response of the overall system, including the fingertip, needs to be considered. The Transfer Function of the whole electro-dynamical system, constituted by the tactile rendering device (the PC, the TI card and the EAP actuator into the support) and the finger of the experimenter, has been thus characterized.

At this aim, the system has been excited with a random signal between 10 Hz and 1000 Hz (frequency range of interest) generated by the MATLAB software and reproduced by the PC sound card. The system response has been measured with the accelerometer fixed on the experimenter fingernail, while the finger was in contact with the vibrating actuator (Figure 4a). In other words, the output acceleration response (measured by the accelerometer on the fingernail) to the input random signal generated by MATLAB has been determined. The Transfer Function has been then computed as the ratio between the Cross Power Spectral Density, between output acceleration and input random signal (CPSDyx), and the Power Spectral Density of the input random signal (PSDx):

$$TF(\omega) = \frac{CPSDyx(\omega)}{PSDx(\omega)} \tag{1}$$

Because the high nonlinearity of the system, and in particular of the finger and its contact with the surface, the Transfer Function has been determined for different values of the normal load between fingertip and actuator, monitored by placing the actuator on the top of the force transducer (Figure 4a). The variation in the obtained Transfer Functions was found to be neglectable in the range between 0.2N and 0.4N (Figure 5), which also coincides with the force range used in the active scanning of the real surfaces. Consequently, it has been decided to fix the normal force at 0.3N during the Transfer Function determination, being this a mean force value within the considered range.

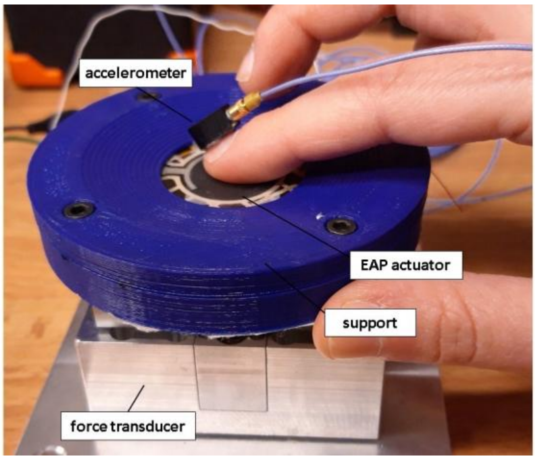


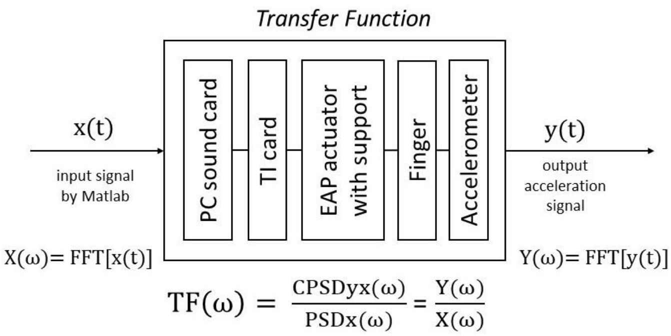


*Figure 4: a) Measurement of acceleration response at the fingernail, with the fingertip in contact with the EAP actuator. The actuator is mounted on the top of the force transducer. b) Definition of the Transfer Function of the system constituted by the tactile rendering device and the finger.*

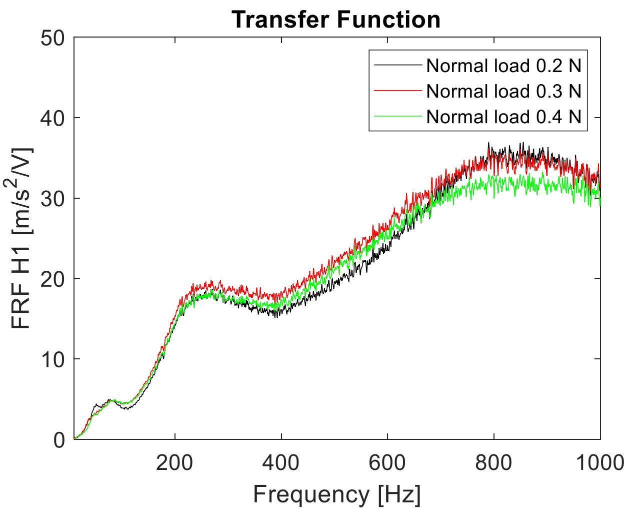


*Figure 5: Comparison of Transfer Functions obtained with normal contact loads of 0.2N, 0.3N and 0.4N.*

### *3.3. FIV signal processing*

The Transfer Function has been then used to process the FIV signal, measured during the sliding of the finger on the real surface, in order to correctly reproduce it by means of the tactile rendering device.

The aim is to find the correct time input signal (as a MATLAB vector) that, given as an input to the tactile rendering device, allows to achieve the reproduction of the FIV signal on the fingernail, when the finger touches the vibrating surface of the EAP actuator. This has been achieved by implementing, in MATLAB, the following signal processing.

Let's define FIV(t) the measured acceleration signal to reproduce, while FIV(ω) is its Fourier Transform (Eq. 2), and TF(ω) is the Transfer Function (Eq. 1), defined in section 3.2.

$$FIV(\omega) = \int_{-\infty}^{+\infty} FIV(t)\, e^{-j\omega t} dt \tag{2}$$

To obtain the input to the tactile device, let's define a new frequency signal Z(ω) as the ratio between the signal FIV(ω) and the Transfer Function TF(ω):

$$\mathrm{Z}(\omega) = \frac{\mathrm{FIV}(\omega)}{\mathrm{TF}(\omega)} \tag{3}$$

Then, the Inverse Fourier Transform of Z(ω) can be calculated as:

$$z(t) = \frac{1}{2\pi} \int_{-\infty}^{+\infty} Z\,(\omega) e^{j\omega t} d\omega \tag{4}$$

The calculated z(t) is then the input time signal to be sent to the tactile device. According to the definition of TF(ω), when z(t) is sent as input to the system (tactile rendering device and finger) the following relation is satisfied in frequency:

$$\mathrm{W}(\omega) = \mathrm{Z}(\omega)\,\mathrm{TF}(\omega) = \left(\frac{\mathrm{FIV}(\omega)}{\mathrm{TF}(\omega)}\right)\mathrm{TF}(\omega) = \mathrm{FIV}(\omega) \tag{5}$$

Thus, the obtained output frequency signal W(ω), i. e. the Fourier Transform of the acceleration measured on the fingernail touching the tactile device, must be equal to the one (FIV(ω)) measured on the fingernail when touching the real surface.

Because the high nonlinearity of the system (finger material properties, contact interface, ….), and because the proposed signal processing uses tools typical of the characterization of linear systems (namely the Transfer Function), it is necessary to verify the reliability of such processing with respect to the effect of the nonlinear contributions. A first verification has been performed directly on the determination of the Transfer Function, with respect to the applied contact force, which effect has been verified to by negligible (Figure 5). In order to account for all the nonlinearities, the validation has been directly obtained by applying the proposed processing to FIV signals.

## 4. Tactile device validation

The validation of the developed tactile device passes by a two-step's validation process:

i. First, the signal processing strategy, to reproduce the FIV stimuli on the finger, by comparing original and mimicked signals;
ii. Then, the possibility to discriminate surface textures, using the reproduced-FIV stimuli operated by the device.

### *4.1. Validation of the signal processing for FIV mimicking*

The correct reproduction of the FIV signal has been verified by comparing the original FIV(t) signal, measured on the fingernail when touching the real surface, with the rendered one, measured when touching the vibro-tactile device. At this aim, the input z(t) signal, recovered by the signal processing described in section 3.3, has been sent as input to the PC sound card, and the output acceleration response has been measured by the accelerometer on the fingernail, while the finger was kept in contact with the vibrating actuator. The finger/actuator normal load was maintained by the experimenter within the defined range (0.2 - 0.4 N).

A scheme of the rendering algorithm and the procedure for the verification of the reproduction of the signal is reported in Figure 6.

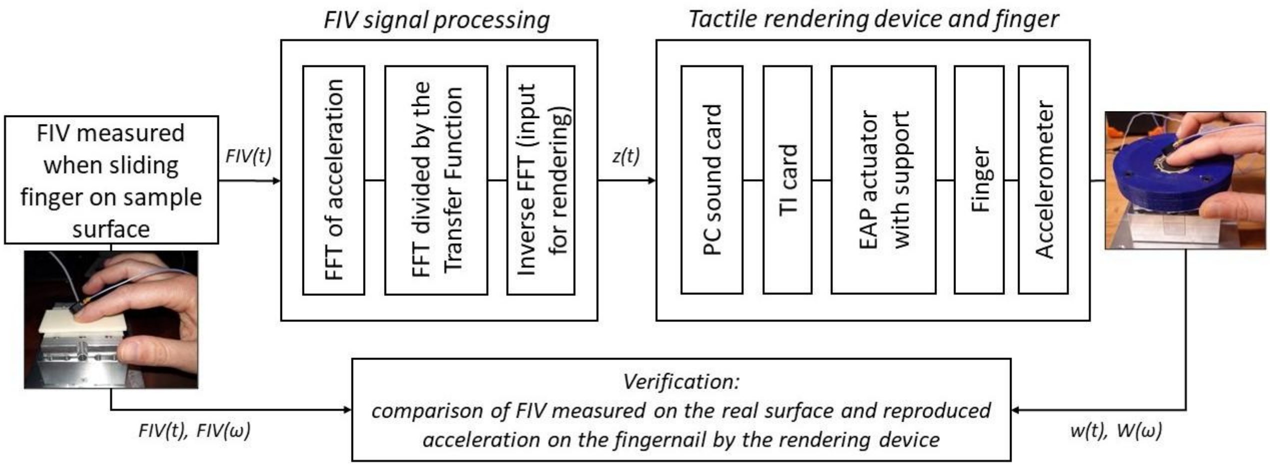


*Figure 6: Scheme of the rendering method and verification procedure.*

Figure 7 shows an example (surface sample S02) of the input signal (red curve), calculated according to the methodology discussed in section 3, and the respective original measured signal (blue curve) on the real surface. Figure 7a shows the comparison between the two frequency spectra, FIV(ω) and Z(ω): the first associated to the original FIV(t) signal, measured when touching the real surface sample S02 (blue curve, FIV(ω)), and the second associated to the input signal z(t) needed to drive the EAP actuator (red curve, Z(ω)) for obtaining the same FIV(t) signal at the fingernail. The input signal for the tactile device is modified according to the shape of the system's Transfer Function (Fig. 7b). For frequencies where the Transfer Function increase, the input for rendering amplitude decrease, with respect to the measured one, and vice versa. Figure 7c shows the comparison between the time signals, which corresponds to the Inverse Fourier Transform z(t) (red curve) and the acceleration measured on the real surface FIV(t) (blue curve), respectively. The input time signal z(t) is then sent to the tactile device in order to obtain the reproduction of the FIV on the fingernail.

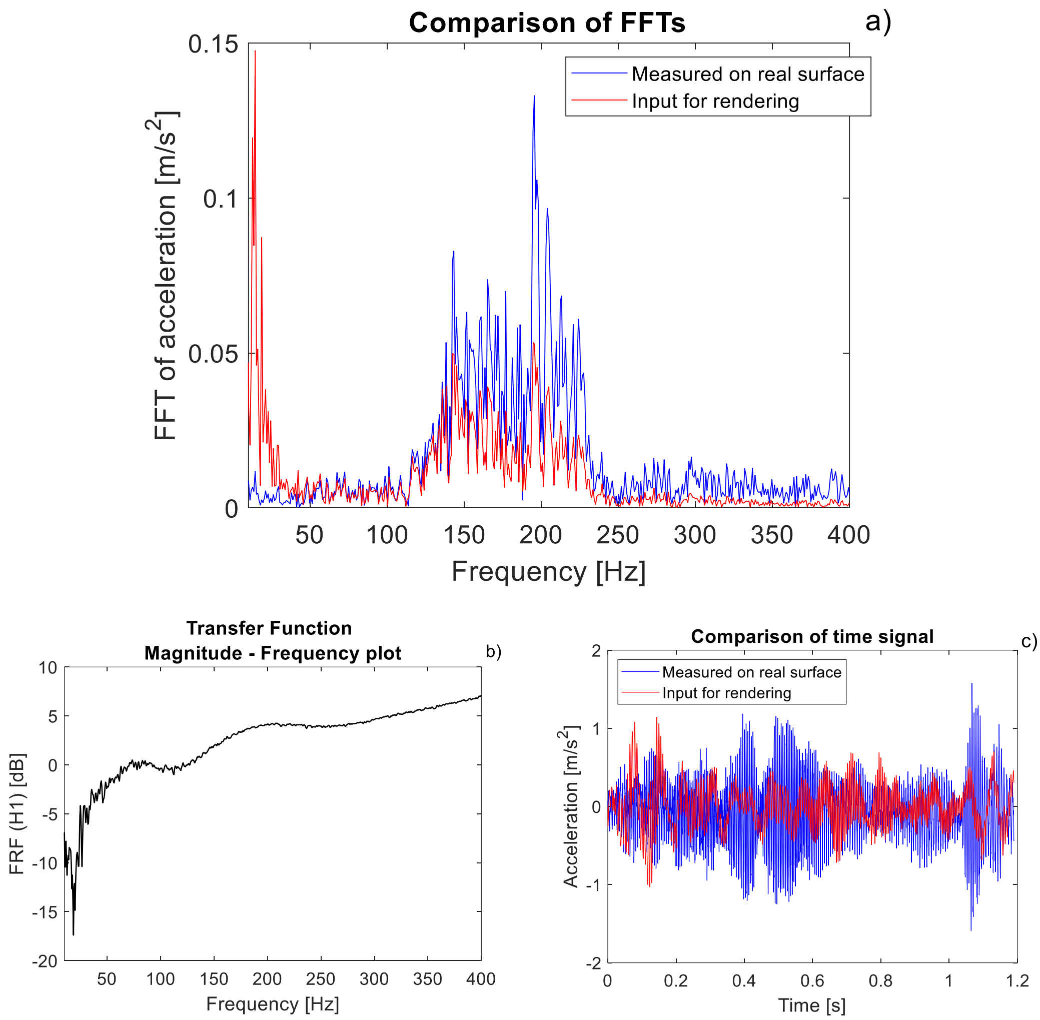


*Figure 7: a) comparison between the spectrum of the FIV measured when touching the real surface and the input signal to drive the tactile device. b) the used Transfer Function to process the signal. c) comparison between the respective time signals.*

The correct reproduction of the signal has been verified by comparing the spectrum of the acceleration measured on the fingernail when exploring the real surface FIV(t) with the one measured when touching the device surface, driven by the z(t) signal.

As an example, Figure 8 shows the comparison between the measured FIV spectra for the texture sample S02. The signals are compared in terms of FFT in Figure 8a and in terms of PSD in Figure 8b. The FIV spectra turned out to be very well reproduced by the tactile device. FFT spectra are very similar (Fig. 8a) and PSD spectra are almost perfectly overlapped (Fig. 8b). Similar behaviours were found for all the tested sample surfaces. As a first validation of the tactile device, these results allow to assert that the device, driven by the signals obtained with the proposed processing technique, is able to correctly reproduce the FIV spectra, measured on the fingernail when touching the tested surfaces.

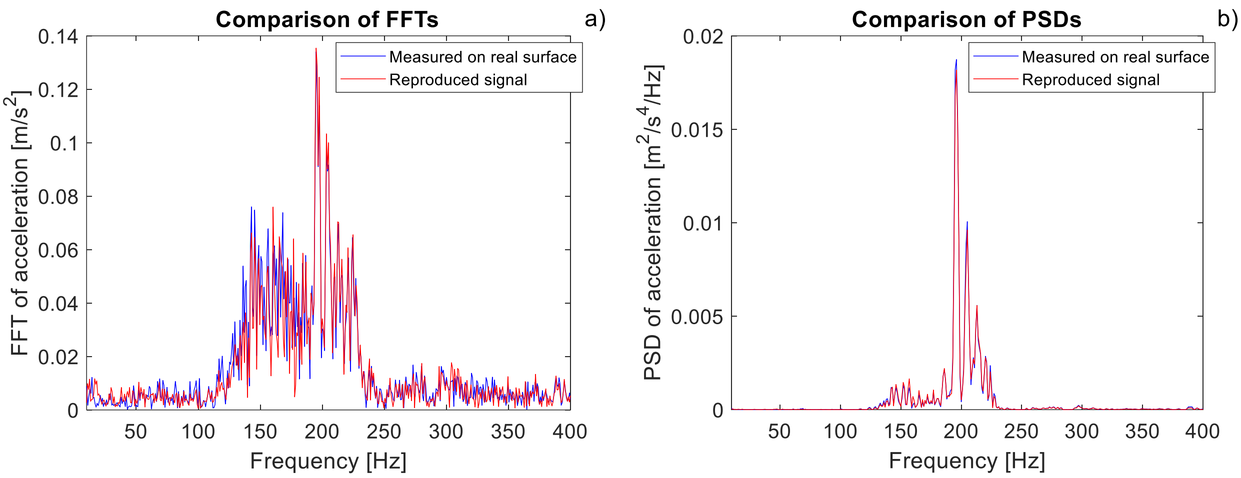


*Figure 8: a) comparison between the FFT of the FIV measured when touching the real surface (S02) and the one measured when touching the tactile device, recovered by the accelerometer on the fingernail. b) comparison between the PSD of the signals.*

## *4.2. Preliminary rendering validation on a discrimination campaign*

A preliminary discrimination campaign on a single subject has been performed in order to provide a preliminary validation of the developed rendering methodology. The aim of the campaign was to evaluate if it is possible to discriminate the surface textures on the basis of the FIV stimuli reproduced by the PIEZOTACT device. The campaign consisted in two different discrimination tasks, the first with the real sample surfaces and the second one with the rendered textures by the tactile device.

Previously, the measurement of FIV and contact forces have been performed, following the protocol described in section 2.4, for all the 12 sample surfaces. Then, the Transfer Function of the tactile rendering device with the subject's finger has been characterized as explained in section 3.2. Finally, the measured FIV signals have been processed with the methodology reported in section 3.3, to obtain the signal for driving the tactile device.

For the discrimination campaign, the surface samples have been divided into 18 sets, each constituted by either 3 or 4 samples (Table 2); the sets were built so that each sample was compared at least once with all the other samples during the campaign.

For each set of samples, a discrimination test has been performed with the real samples and another one has been performed with the respective rendered textures, simulated by the tactile device. This means the subject performed 18 consecutive tests, each test constituted by a discrimination of 3 or 4 real samples and a discrimination of the corresponding simulated ones by the device. The overall duration of the tests, about 1 hour, was split in intervals shorter than 20 minutes, in order to avoid fatigue of the subject and lost in performance.

For each set of samples, the first discrimination test involved only the real surfaces. The test with the real surfaces was necessary to evaluate the capability of the subject to discriminate the real textures. In the first instance, the subject (male, 41 years old) could freely explore the real textures to acquire familiarity with their tactile perception. In this phase the subject could touch the surfaces and read the sample numbers (printed on the back side of the samples), learning to associate to each perceived texture the corresponding number. Then, the subject was blindfolded and equipped with earmuff. The samples were presented in a random order to the subject, who was not aware about the order. Then, the subject had to touch and discriminate the samples, by associating each sample to the correct number, entrusting only with the tactile sense.

The second discrimination test involved the simulated surfaces (reproduced FIV signals) by the PIEZOTACT device. For each set of samples (constituted by 3 or 4 samples), a random sequence of simulated surfaces has been defined, also with repetitions of the same surface, in order to prevent the remaining samples to be recognized by exclusion by the subject (each sequence was constituted by 5 or 6 simulated textures by the PIEZOTACT, in a random order). The random sequence of simulated surfaces has been presented to the subject; it was asked to the subject to touch the vibrating EAP actuator and to associate to each rendered texture the corresponding real one, declaring each surface’s number. During the test, the subject could touch the set of real samples to compare the real and simulated surfaces. The subject was also allowed to perceive the sequence of simulated surfaces more than once, and the test was declared as finished when the subject was satisfied by its answers (no time limit has been imposed to the subject to perform the discrimination task). The subject wore earmuff to avoid the acoustic feedback by the actuator.

The results (answers) of both the discrimination tasks, the one with real surfaces and the one with the simulated ones, have been collected and analysed by means of association matrices. On the horizontal plane of the matrix, the x-axis shows the tested samples and the y-axis reports the answers declared by the subject. This means that the correct associations of the samples are localized on the principal diagonal of the matrix, while the associations out from the diagonal represent the discrimination errors. The vertical axis shows the percentage of associations. The percentage of association was computed as the number of times each association appeared in the whole test, normalized with respect to the number of times each sample was presented to the subject, expressed in percentage.

*Table 2: Sets of samples used for the discrimination campaign. Each set is constituted by 3 or 4 samples.*

| Set | Samples | Set | Samples |
|---|---|---|---|
| A | S01, S08, S10 | L | S03, S06, S01 |
| B | S11, S09, S12 | M | S01, S05, S09 |
| C | S04, S02, S03 | N | S08, S09, S07, S03 |
| D | S06, S07, S05, S11 | O | S12, S08, S04, S06 |
| E | S01, S11, S04 | P | S06, S09, S02 |
| F | S08, S11, S02 | Q | S02, S10, S05, S12 |
| G | S10, S11, S03 | R | S04, S07, S05 |
| H | S10, S09, S04 | S | S08, S05, S03, S12 |
| I | S12, S07, S01, S02 | T | S10, S07, S06 |

Figure 9 shows the results of both the campaigns. Both in the case of the real textures (Fig. 9a) and the simulated ones (Fig. 9b), the greatest percentages of correlation can be found on the principal diagonal of the association matrix. This result denotes an extremely good discrimination performance of the subject in both the discrimination campaigns.

Moreover, there is a good agreement between the results obtained when discriminating real and simulated surfaces. Indeed, the most frequent discrimination errors occurred in the tests with the simulated surfaces have been recovered in the case of the real ones too.  This behaviour has been ascribed to similarities in the frequency distribution of the FIV signals associated to the surfaces, resulting in discrimination errors, both for real and simulated samples. As a confirmation of such hypothesis, in the cases of wrong discrimination, the FIV spectra, measured when touching the real surfaces and reproduced by the tactile device, are very close each other, justifying the errors in the discrimination of both the real and the simulated surfaces.

Figure 10a reports, as an example, the samples labelled S07, S05 and S12, which are characterized by very similar FIV spectra. These samples have been frequently confused, both in the cases of the real and simulated surfaces. In particular, the samples S07 and S05 have a very similar topographic parameters (Table 1) and FIV characteristic spectra, and they resulted hard to discriminate both for real and simulated surfaces.

On the contrary, the samples S08 and S04 show different FIV spectra (Fig. 10b) and they never got confused during the campaign.

In conclusion, the presented tactile device, reproducing accurately the FIV stimuli, gave a good result in terms of discrimination of simulated textures, in agreement with the discrimination of the real touched surfaces.

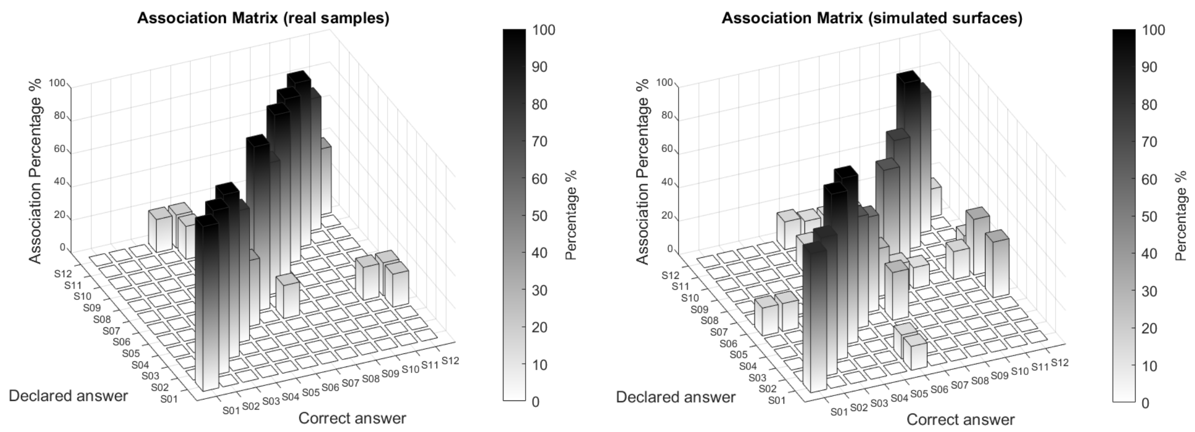


*Figure 9: Results of the discrimination campaign. a) association matrix obtained with the real samples. b) association matrix obtained with the rendered surfaces with the PIEZOTACT.*

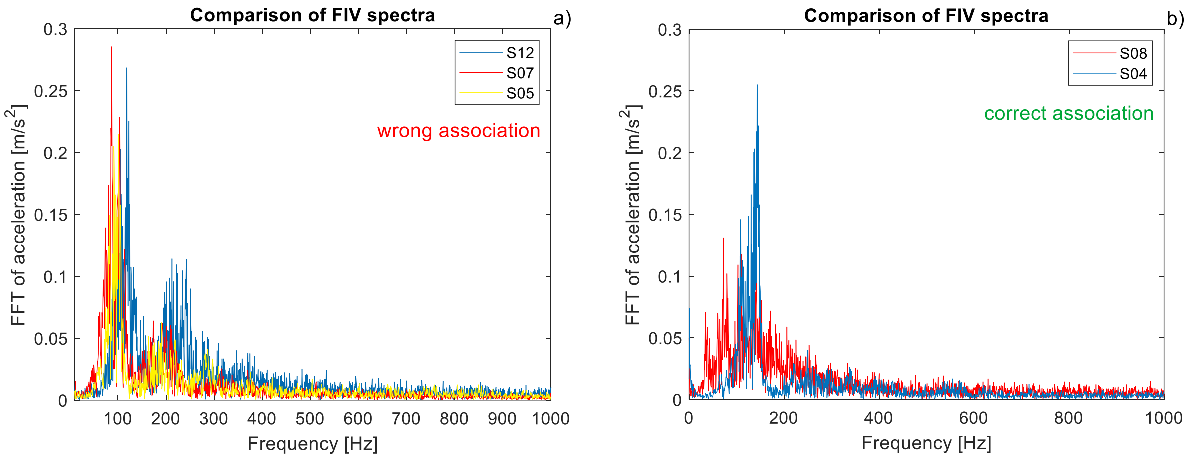


*Figure 10: Examples of FIV spectra in case of wrong (a) and correct (b) discrimination.*

## 5. Conclusions

The simulation of tactile perception passes through the identification and mimicking of the mechanical stimuli at the origin of touch. In this work, a tactile device, named PIEZOTACT, for simulating surface textures by the reproduction of the Friction-Induced Vibrations, has been presented. The Friction-Induced Vibrations measured when exploring the real surfaces have been reproduced by a light, thin and flexible Electro-Active Polymer actuator. A signal processing strategy, exploiting the system Transfer Function, has been developed in order to reproduce on the fingernail the same vibration spectra measured when exploring the real surfaces.

In order to validate the device and the proposed signal processing, the spectra of the accelerations (FIV) measured when touching the EAP actuator were compared with the ones measured when exploring the real surfaces. The proposed method resulted to be suitable to correctly reproduce the FIV spectra by the PIEZOTACT. In fact, the simulated FIV stimuli were almost overlapping the ones measured on the real surfaces.

Finally, a preliminary discrimination campaign has been performed by a single subject to evaluate if it was possible to discriminate the surface textures on the basis of the FIV reproduced by the device. The subject was able to correctly discriminate the textures with a reduced number of association errors. Moreover, the few errors, recovered when testing by the simulated textures, were similarly obtained with the real surfaces. These errors in the discrimination of the tested textures have been explained by the similarity in the spectra of the FIV stimuli, highlighting the main role played by the Friction-Induced Vibrations in the perception of surface textures.

## Bibliography

[1] C. Basdogan, F. Giraud, V. Levesque and S. Choi, "A Review of Surface Haptics: Enabling Tactile Effects on Touch Surfaces", in IEEE Transactions on Haptics, vol. 13, no. 3, pp. 450-470, 1 July-Sept. 2020, doi: 10.1109/TOH.2020.2990712.

[2] A. Costes, F. Danieau, F. Argelaguet, P. Guillotel and A. Lécuyer, "Towards Haptic Images: A Survey on Touchscreen-Based Surface Haptics," in IEEE Transactions on Haptics, vol. 13, no. 3, pp. 530-541, 1 July-Sept. 2020, doi: 10.1109/TOH.2020.2984754.

[3] Jones LA, Sarter NB. “Tactile Displays: Guidance for Their Design and Application”. *Human Factors*. 2008;50(1):90-111. doi:10.1518/001872008X250638

[4] S. Choi and K. J. Kuchenbecker, "Vibrotactile Display: Perception, Technology, and Applications", in Proceedings of the IEEE, vol. 101, no. 9, pp. 2093-2104, Sept. 2013, doi: 10.1109/JPROC.2012.2221071.

[5] Haghighi Osgouei, Reza. (2020). Electrostatic Friction Displays to Enhance Touchscreen Experience. 10.5772/intechopen.91056.

[6] J. M. Romano and K. J. Kuchenbecker, "Creating Realistic Virtual Textures from Contact Acceleration Data," in IEEE Transactions on Haptics, vol. 5, no. 2, pp. 109-119, April-June 2012, doi: 10.1109/TOH.2011.38.

[7] H. Culbertson, J. Unwin and K. J. Kuchenbecker, "Modeling and Rendering Realistic Textures from Unconstrained Tool-Surface Interactions," in IEEE Transactions on Haptics, vol. 7, no. 3, pp. 381-393, 1 July-Sept. 2014, doi: 10.1109/TOH.2014.2316797.

[8] Abdulali A., Jeon S. (2018) Data-Driven Rendering of Anisotropic Haptic Textures. In: Hasegawa S., Konyo M., Kyung KU., Nojima T., Kajimoto H. (eds) Haptic Interaction. AsiaHaptics 2016. Lecture Notes in Electrical Engineering, vol 432. Springer, Singapore. https://doi.org/10.1007/978-981-10-4157-0_67

[9] A. M. Okamura, J. T. Dennerlein and R. D. Howe, "Vibration feedback models for virtual environments," Proceedings. 1998 IEEE International Conference on Robotics and Automation (Cat. No.98CH36146), Leuven, Belgium, 1998, pp. 674-679 vol.1, doi: 10.1109/ROBOT.1998.677050.

[10] S. Shin, R. H. Osgouei, K. Kim and S. Choi, "Data-driven modeling of isotropic haptic textures using frequency-decomposed neural networks," 2015 IEEE World Haptics Conference (WHC), Evanston, IL, 2015, pp. 131-138, doi: 10.1109/WHC.2015.7177703.

[11] Paul Strohmeier and Kasper Hornbæk. 2017. Generating Haptic Textures with a Vibrotactile Actuator. In Proceedings of the 2017 CHI Conference on Human Factors in Computing Systems (CHI '17). Association for Computing Machinery, New York, NY, USA, 4994–5005. DOI:https://doi.org/10.1145/3025453.3025812

[12] J. Jiao et al., "Data-driven rendering of fabric textures on electrostatic tactile displays," 2018 IEEE Haptics Symposium (HAPTICS), San Francisco, CA, 2018, pp. 169-174, doi: 10.1109/HAPTICS.2018.8357171.

[13] R. H. Osgouei, J. R. Kim and S. Choi, "Data-Driven Texture Modeling and Rendering on Electrovibration Display," in IEEE Transactions on Haptics, vol. 13, no. 2, pp. 298-311, 1 April-June 2020, doi: 10.1109/TOH.2019.2932990.

[14] R. H. Osgouei, S. Shin, J. R. Kim and S. Choi, "An inverse neural network model for data-driven texture rendering on electrovibration display," 2018 IEEE Haptics Symposium (HAPTICS), San Francisco, CA, 2018, pp. 270-277, doi: 10.1109/HAPTICS.2018.8357187.

[15] S. Rasool and A. Sourin, "Image-Driven Haptic Rendering in Virtual Environments," 2013 International Conference on Cyberworlds, Yokohama, 2013, pp. 286-293, doi: 10.1109/CW.2013.28.

[16] Wu, S., Sun, X., Wang, Q. et al. Tactile modeling and rendering image-textures based on electrovibration. Vis Comput 33, 637–646 (2017). https://doi.org/10.1007/s00371-016-1214-3.

[17] Olivier Bau, Ivan Poupyrev, Ali Israr, and Chris Harrison. 2010. TeslaTouch: electrovibration for touch surfaces. In Proceedings of the 23nd annual ACM symposium on User interface software and technology (UIST '10). Association for Computing Machinery, New York, NY, USA, 283–292. DOI:https://doi.org/10.1145/1866029.1866074

[18] Bueno M-A, Lemaire-Semail B, Amberg M, Giraud F. A simulation from a tactile device to render the touch of textile fabrics: a preliminary study on velvet. Textile Research Journal. 2014;84(13):1428-1440. doi:10.1177/0040517514521116

[19] T. Watanabe and S. Fukui, "A method for controlling tactile sensation of surface roughness using ultrasonic vibration," Proceedings of 1995 IEEE International Conference on Robotics and Automation, Nagoya, Japan, 1995, pp. 1134-1139 vol.1, doi: 10.1109/ROBOT.1995.525433.

[20] M. Wiertlewski, R. F. Friesen and J. E. Colgate, "Partial squeeze film levitation modulates fingertip friction", Proc. Nat. Acad. Sci., vol. 113, no. 33, pp. 9210-9215, 2016.

[21] B. Camillieri, M.-A. Bueno, M. Fabre, B. Juan, B. Lemaire-Semail and L. Mouchnino, "From finger friction and induced vibrations to brain activation: Tactile comparison between real and virtual textile fabrics", Tribology Int., vol. 126, pp. 283-296, 2018.

[22] Wiertlewski M., Leonardis D., Meyer D.J., Peshkin M.A., Colgate J.E. (2014) A High-Fidelity Surface-Haptic Device for Texture Rendering on Bare Finger. In: Auvray M., Duriez C. (eds) Haptics:

Neuroscience, Devices, Modeling, and Applications. EuroHaptics 2014. Lecture Notes in Computer Science, vol 8619. Springer, Berlin, Heidelberg. https://doi.org/10.1007/978-3-662-44196-1_30

[23] G. Liu, C. Zhang and X. Sun, "Tri-Modal Tactile Display and Its Application Into Tactile Perception of Visualized Surfaces," in IEEE Transactions on Haptics, vol. 13, no. 4, pp. 733-744, Oct.-Dec. 2020, doi: 10.1109/TOH.2020.2979182.

[24] H. Culbertson and K. J. Kuchenbecker, "Importance of Matching Physical Friction, Hardness, and Texture in Creating Realistic Haptic Virtual Surfaces," in IEEE Transactions on Haptics, vol. 10, no. 1, pp. 63-74, 1 Jan.-March 2017, doi: 10.1109/TOH.2016.2598751.

[25] J. Jiao, Y. Zhang, D. Wang, X. Guo and X. Sun, "HapTex: A Database of Fabric Textures for Surface Tactile Display," 2019 IEEE World Haptics Conference (WHC), Tokyo, Japan, 2019, pp. 331-336, doi: 10.1109/WHC.2019.8816167.

[26] H. Culbertson, J. J. López Delgado and K. J. Kuchenbecker, "One hundred data-driven haptic texture models and open-source methods for rendering on 3D objects," 2014 IEEE Haptics Symposium (HAPTICS), Houston, TX, 2014, pp. 319-325, doi: 10.1109/HAPTICS.2014.6775475.

[27] M. Strese, J. Lee, C. Schuwerk, Q. Han, H. Kim and E. Steinbach, "A haptic texture database for tool-mediated texture recognition and classification," 2014 IEEE International Symposium on Haptic, Audio and Visual Environments and Games (HAVE) Proceedings, Richardson, TX, 2014, pp. 118-123, doi: 10.1109/HAVE.2014.6954342.

[28] D. Katz, The world of touch, L. Erlbaum, 1925 - 1989.

[29] Hollins M, Bensmaïa S, Risner R. The duplex theory of tactile texture perception. In: Proceedings of fourteenth annual meeting of the international society for psychophysics; 1998.

[30] Lederman SJ, Klatzky RL. Haptic perception: a tutorial. In: Attention, perception. & Psychophysics; 2009. p. 1439–59.

[31] Bensmaïa, S., Hollins, M. Pacinian representations of fine surface texture. *Perception & Psychophysics* **67,** 842–854 (2005).

[32] Sliman J. BensmaÏa & Mark Hollins (2003) The vibrations of texture, Somatosensory & Motor Research, 20:1, 33-43.

[33] Fagiani R, Massi F, Chatelet E, Berthier Y, Akay A. Tactile perception by friction induced vibrations. Tribol Int 2011; 44:1100–10.

[34] J. Dacleu Ndengue et al., "Tactile Perception and Friction-Induced Vibrations: Discrimination of Similarly Patterned Wood-Like Surfaces," in IEEE Transactions on Haptics, vol. 10, no. 3, pp. 409-417, 1 July-Sept. 2017, doi: 10.1109/TOH.2016.2643662.

[35] M. Di Bartolomeo, F. Morelli, D. Tonazzi, F. Massi, Y. Berthier, Investigation of the role of contact-induced vibrations in tactile discrimination of textures, Mechanics & Industry, 18 (4) 404 (2017).

[36] I. Cesini, J. D. Ndengue, E. Chatelet, J. Faucheu, F. Massi, Correlation between friction-induced vibrations and tactile perception during exploration tasks of isotropic and periodic textures, Tribology International, 2018, 120(330-339).

[37] Fagiani, R., Massi, F., Chatelet, E. *et al.* Contact of a Finger on Rigid Surfaces and Textiles: Friction Coefficient and Induced Vibrations. *Tribol Lett* **48,** 145–158 (2012).

[38] V. Massimiani, B. Weiland, E. Chatelet, P.H. Cornuault, J. Faucheu, F. Massi, The role of mechanical stimuli on hedonistic and topographical discrimination of textures, Tribology International, 2020, 143.

[39] Jiyong Hu, Xiaofeng Zhang, Xudong Yang, Ruitao Jiang, Xin Ding & Rubin Wang (2016) Analysis of fingertip/fabric friction-induced vibration signals toward vibrotactile rendering, The Journal of The Textile Institute, 107:8, 967-975, DOI: 10.1080/00405000.2015.1077011

[40] Greenspon Charles M., McLellan Kristine R., Lieber Justin D. and Bensmaia Sliman J. 2020Effect of scanning speed on texture-elicited vibrationsJ. R. Soc. Interface.1720190892.

[41] Delhaye B, Hayward V, Lefèvre P and Thonnard J-L (2012) Texture-induced vibrations in the forearm during tactile exploration. Front. Behav. Neurosci. 6:37. doi: 10.3389/fnbeh.2012.00037

[42] Jiang, R., Hu, J., Yang, X. et al. Analysis of fingertip/textile friction-induced vibration by time-frequency method. Fibers Polym 17, 630–636 (2016).

[43] Zhou, Xue & Mo, Ji & Li, Yi & Xiang, Zaiyu & Yang, Dan & Masen, Marc & Jin, Zhong. (2020). Effect of Finger Sliding Direction on Tactile Perception, Friction and Dynamics. Tribology Letters. 68. 10.1007/s11249-020-01325-6.

[44] Christian Frisson, Julien Decaudin, Thomas Pietrzak, Alexander Ng, Pauline Poncet, Fabrice Casset, Antoine Latour, and Stephen A. Brewster. 2017. Designing Vibrotactile Widgets with Printed Actuators and Sensors. In Adjunct Publication of the 30th Annual ACM Symposium on User Interface Software and Technology (UIST '17). Association for Computing Machinery, New York, NY, USA, 11–13. DOI:https://doi.org/10.1145/3131785.3131800

[45] Poncet, P.; Casset, F.; Latour, A.; Domingues Dos Santos, F.; Pawlak, S.; Gwoziecki, R.; Devos, A.; Emery, P.; Fanget, S. Static and Dynamic Studies of Electro-Active Polymer Actuators and Integration in a Demonstrator. Actuators 2017, 6, 18.

[46] P. Poncet et al., "Design and realization of electroactive polymer actuators for transparent and flexible haptic feedback interfaces," 2016 17th International Conference on Thermal, Mechanical and Multi-Physics Simulation and Experiments in Microelectronics and Microsystems (EuroSimE), Montpellier, France, 2016, pp. 1-5, doi: 10.1109/EuroSimE.2016.7463310.

[47] Faucheu J., Weiland B., Juganaru-Mathieu M., Witt A., Cornuault P-H., "Tactile aesthetics: textures that we like or hate to touch", *Acta Psychologica*, 201 (2019). https://doi.org/10.1016/j.actpsy.2019.102950